IEEE Photonics Journal
An IEEE Photonics Society Publication

Performance Analysis of Mixed Nakagami-*m* and Gamma–Gamma Dual-Hop FSO Transmission Systems

Volume 7, Number 1, February 2015

Emna Zedini, Student Member, IEEE
Imran Shafique Ansari, Student Member, IEEE
Mohamed-Slim Alouini, Fellow, IEEE

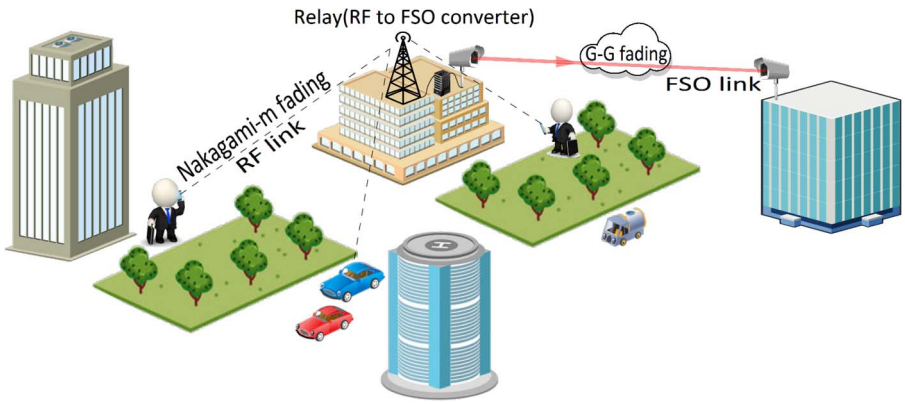

DOI: 10.1109/JPHOT.2014.2381657
1943-0655 © 2014 IEEE

Performance Analysis of Mixed Nakagami-*m* and Gamma–Gamma Dual-Hop FSO Transmission Systems

Emna Zedini, *Student Member, IEEE*,
Imran Shafique Ansari, *Student Member, IEEE*, and
Mohamed-Slim Alouini, *Fellow, IEEE*

Computer, Electrical, and Mathematical Sciences and Engineering Division, King Abdullah University of Science and Technology, Thuwal 23955-6900, Saudi Arabia

DOI: 10.1109/JPHOT.2014.2381657

Manuscript received October 16, 2014; revised November 30, 2014; accepted December 5, 2014. Date of publication December 18, 2014; date of current version January 6, 2015. This work was supported in part by a grant from King Abdulaziz City for Science and Technology. Corresponding author: E. Zedini (e-mail: emna.zedini@kaust.edu.sa).

Abstract: In this paper, we carry out a unified performance analysis of a dual-hop relay system over the asymmetric links composed of both radio-frequency (RF) and unified free-space optical (FSO) links under the effect of pointing errors. Both fixed and variable gain relay systems are studied. The RF link is modeled by the Nakagami-*m* fading channel and the FSO link by the Gamma–Gamma fading channel subject to both types of detection techniques (i.e., heterodyne detection and intensity modulation with direct detection). In particular, we derive new unified closed-form expressions for the cumulative distribution function, the probability density function, the moment generating function (MGF), and the moments of the end-to-end signal-to-noise ratio (SNR) of these systems in terms of the Meijer's *G* function. Based on these formulas, we offer exact closed-form expressions for the outage probability (OP), the higher order amount of fading, and the average bit error rate (BER) of a variety of binary modulations in terms of the Meijer's *G* function. Furthermore, an exact closed-form expression of the end-to-end ergodic capacity is derived in terms of the bivariate *G* function. Additionally, by using the asymptotic expansion of the Meijer's *G* function at the high-SNR regime, we derive new asymptotic results for the OP, the MGF, and the average BER in terms of simple elementary functions.

Index Terms: Free-space optics (FSO), mixed RF/FSO systems, nakagami-*m* fading, atmospheric turbulence, pointing errors, outage probability (OP), bit error rate (BER), ergodic capacity, Meijer's *G* function.

1. Introduction

Optical communication through the atmosphere, also known as free-space optical (FSO) communication, has attracted considerable research attention recently as a cost effective and wide bandwidth solution operating at the unlicensed optical spectrum, relative to the traditional radio frequency (RF) transmission [1]–[5]. Moreover, FSO communications offer high data rates, and are utilized for a variety of applications such as, fiber backup, back-haul for wireless cellular networks, enterprise/local area network connectivity, metropolitan area network extensions, redundant link, and disaster recovery [6]. However, inhomogeneities induced by the temperature and

atmospheric pressure in the FSO links cause fluctuations in the refractive index. This impairment caused by the atmospheric effects is known as the atmospheric turbulence [2]. In this context, we investigate in our analysis the effects of weak, moderate, and strong turbulence regimes on the overall system performance. Another major impairment over FSO links is building sway caused by thermal expansion, wind loads, and weak earthquakes [7], [8]. This phenomenon leads to a misalignment between the transmitter and the receiver, also known as pointing error that severely degrades the channel performance [1], [9]. In addition, it is worthy to learn that the main type of detection technique in FSO systems is IM/DD. Coherent modulation is recently employed as an alternative detection approach. Despite of the complexity of implementing coherent receivers relative to IM/DD systems, heterodyne detection that belongs to coherent mode offers better performance in overcoming turbulence effects [10], [11].

Relaying technique has gained an enormous interest due to its advantages including not only wider and energy-efficient coverage but also increased capacity in the wireless communication systems. Recently, several efforts have been conducted to investigate the relay system performance under various fading conditions [12]–[15]. Moreover, literature regarding the asymmetric relay networks based on both RF as well as FSO characteristics includes [16]–[20]. Reference [20] investigates a multiuser dual-hop relaying system over mixed RF/FSO links. In [16], the performance analysis of asymmetric dual-hop RF-FSO relay system is presented. In [18], the performance analysis of a dual-hop variable gain relay RF-unified FSO transmission system subject to pointing errors is presented. Reference [17] investigates the performance of a dual-branch fixed gain relay RF-FSO transmission system under the effect of pointing errors and subject to both types of detection techniques (i.e., IM/DD as well as heterodyne detection). However, the results presented in [17] were derived under the assumption of a non light of sight (NLOS) Rayleigh fading in the RF link, and as such does not cover the case when a line of sight (LOS) component is present between the source and relay. Since the Rician and Nakagami-*m* fading models are more appropriate for propagation environments in LOS communications [21], we, for the first time, present and study the performance of asymmetric dual-hop relay transmission system with mixed Nakagami-*m*/unified FSO links. More specifically, the FSO link is assumed to be operating over unified Gamma–Gamma fading environment [1], [3], [4], [10], [11], [22]–[26] under the effect of pointing errors, and the RF link over Nakagami-*m* fading that includes the Rayleigh fading as a special case. In this context and in our performance analysis study, we consider both fixed and variable relay schemes. Results for the fixed gain relaying were made public in [27]. We present unified approach for the derivation of the cumulative distribution function (CDF), the probability density function (PDF), the moment generating function (MGF), the moments, the higher-order amount of fading (AF), the outage probability (OP), and the average bit-error rate (BER) of a binary modulation scheme in terms of the Meijer's *G* function. Additionally, we present the ergodic capacity in terms of the bivariate *G* function. Further, we introduce the asymptotic expressions for all the expressions derived earlier in terms of the Meijer's *G* function at high signal-to-noise ratio (SNR) regime.

The remainder of the paper is organized as follows. In Section 2, the system model for both fixed and variable gain relay schemes is introduced. Exact closed-form results for the PDF, the CDF, the MGF, the moments, the AF, the OP, the BER, and the ergodic capacity followed by asymptotic expressions are presented in Section 3. The derived analytical expressions in the previous sections are numerically evaluated and interpreted in Section 4. Finally, we review our main results and we draw some conclusions in Section 5.

2. Asymmetric Nakagami-*m*/Unified FSO Relay Transmission Systems With Fixed Gain Relay

2.1. Channel and System Models

We consider an asymmetric dual-hop amplify-and-forward relaying system where the source node S and the destination node D are communicating through an intermediate relay node R,

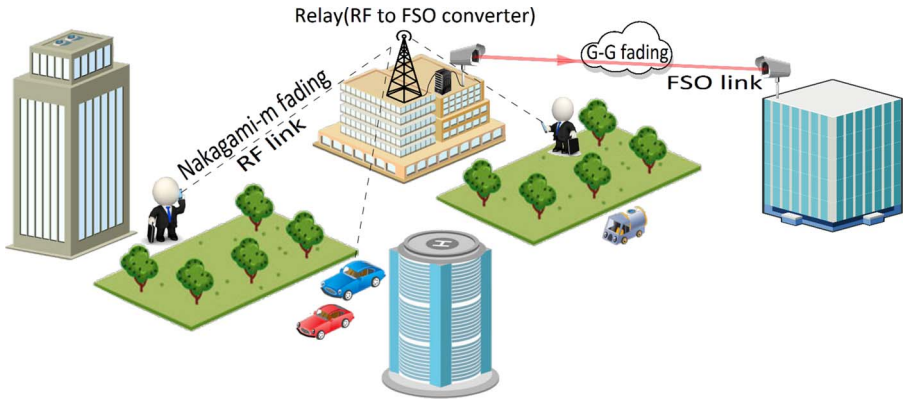

Fig. 1. RF-FSO dual-hop system.

as shown in Fig. 1. As can be seen from Fig. 1, multiple RF users can be multiplexed (MUX) to combine and be sent over the FSO link that is considered to be very high in terms of bandwidth (BW). This being an initial study with such a channel model, we analyze the system for a single random user. The RF point-to-point propagation link (i.e., S–R link) is assumed to follow a Nakagami-*m* distribution. On the other hand, we assume the second FSO link (i.e., R–D link) experiences unified Gamma–Gamma fading with pointing error impairments.

In the fixed gain relaying scheme, the end-to-end SNR can be expressed as [12]

$$\gamma = \frac{\gamma_1 \gamma_2}{\gamma_2 + C} \tag{1}$$

where γ_1 denotes the SNR of the RF S–R hop, γ_2 represents the SNR of the FSO R–D hop, and C stands for a fixed relay gain [12], [16].

In this paper, we assume that the RF S–R link experiences Nakagami-*m* fading distribution with the probability density function (PDF) in [21]

$$f_{\gamma_1}(\gamma_1) = \left(\frac{m}{\Omega}\right)^m \frac{\gamma_1^{m-1}}{\Gamma(m)} \exp\left(-\frac{m}{\Omega}\gamma_1\right) \tag{2}$$

where m is the Nakagami-*m* fading parameter $(m \geq 1/2)$, $\Gamma(\cdot)$ is the Gamma function as defined in [23, Eq. (8.310)] and Ω represents the average fading power, i.e., $\Omega = \mathbb{E}_{\gamma_1}[\gamma_1]$ with $\mathbb{E}[\cdot]$ denoting the expectation operator. It is worthy to note that the PDF in (2) includes the Rayleigh distribution ($m = 1$) as a special case.

The FSO R–D link is assumed to follow a unified Gamma–Gamma fading distribution with pointing error impairments for which the PDF of the SNR is given by [29]

$$f_{\gamma_2}(\gamma_2) = \frac{\xi^2}{r\gamma_2 \Gamma(\alpha)\Gamma(\beta)} \mathrm{G}_{1,3}^{3,0}\left[h\alpha\beta \left(\frac{\gamma_2}{\mu_r}\right)^{\frac{1}{r}} \middle| \begin{matrix} \xi^2 + 1 \\ \xi^2, \alpha, \beta \end{matrix} \right] \tag{3}$$

where r is the parameter specifying the detection technique type (i.e., $r = 1$ accounts for heterodyne detection and $r = 2$ represents IM/DD), $h = \xi^2/(\xi^2 + 1)$, ξ denotes the ratio between the equivalent beam radius at the receiver and the pointing error displacement standard deviation (jitter) at the receiver [1], [22] (i.e., for negligible pointing errors, $\xi \to \infty$), α and β are the fading/scintillation parameters related to the atmospheric turbulence conditions with small values of these two parameters pointing to severe fading conditions [4], [9], $\mathrm{G}_{\cdot,\cdot}^{\cdot,\cdot}(\cdot)$ is the Meijer's G function as defined in [28, Eq. (9.301)], and μ_r standing for the average electrical SNR. More specifically, for μ_r, when $r = 1$, $\mu_1 = \mu_{\text{heterodyne}} = \mathbb{E}[\gamma_2] = \overline{\gamma}_2$ and when $r = 2$, $\mu_2 = \mu_{\text{IM/DD}} = \overline{\gamma}_2 \alpha\beta\xi^2 \times (\xi^2 + 2)/[(\alpha + 1)(\beta + 1)(\xi^2 + 1)^2]$.

2.2. Statistical Characteristics

2.2.1. Cumulative Distribution Function

The CDF of γ is given by

$$F_\gamma(\gamma) = \Pr\left[\frac{\gamma_1\gamma_2}{\gamma_2 + C} < \gamma\right] \tag{4}$$

which can be expressed as

$$\begin{aligned} F_\gamma(\gamma) &= \int_0^\infty \Pr\left[\frac{\gamma_1\gamma_2}{\gamma_2 + C} < \gamma | \gamma_2\right] f_{\gamma_2}(\gamma_2) d\gamma_2 \\ &= 1 - \frac{\xi^2}{r\Gamma(\alpha)\Gamma(\beta)\Gamma(m)} \int_0^\infty \frac{1}{\gamma_2} \Gamma\left(m, \frac{m\gamma(\gamma_2 + C)}{\Omega\gamma_2}\right) \mathrm{G}_{1,3}^{3,0}\left[h\alpha\beta\left(\frac{\gamma_2}{\mu_r}\right)^{\frac{1}{r}} \middle| \begin{matrix} \xi^2 + 1 \\ \xi^2, \alpha, \beta \end{matrix}\right] d\gamma_2. \end{aligned} \tag{5}$$

To the best of the authors' knowledge, the solution to the integral in (5) is not available in exact closed-form nor in terms of the extended generalized bivariate Meijer's *G* function (EGBMGF) because of the shift in the incomplete Gamma function. Therefore, we utilize the finite series representation of the incomplete Gamma function in [28, Eq. (8.352.7)] to rewrite $\Gamma(m, (m\gamma(\gamma_2 + C)/\Omega\gamma_2))$ as $(m-1)!\exp(-(m\gamma/\Omega))\exp(-(mC\gamma/\Omega\gamma_2))\sum_{k=0}^{m-1}(1/k!)(m\gamma/\Omega)^k(1 + (C/\gamma_2))^k$. Since the summation is upper limited by *m*, our results are restricted to the case of Nakagami-*m* with integer values of *m*. Further using the binomial expansion in [28, Eq. (1.111)], $(1 + (C/\gamma_2))^k$ can be expressed as $\sum_{j=0}^{k}\binom{k}{j}(C/\gamma_2)^j$. Therefore, the CDF in (5) can be determined as

$$\begin{aligned} F_\gamma(\gamma) = 1 - \frac{\xi^2(m-1)!\exp\left(-\frac{m\gamma}{\Omega}\right)}{r\Gamma(\alpha)\Gamma(\beta)\Gamma(m)} \sum_{k=0}^{m-1}\frac{1}{k!}\left(\frac{m\gamma}{\Omega}\right)^k \sum_{j=0}^{k}\binom{k}{j}C^j \\ \times \int_0^\infty \gamma_2^{-j-1}\exp\left(-\frac{m\gamma C}{\Omega\gamma_2}\right)\mathrm{G}_{1,3}^{3,0}\left[h\alpha\beta\left(\frac{\gamma_2}{\mu_r}\right)^{\frac{1}{r}} \middle| \begin{matrix} \xi^2 + 1 \\ \xi^2, \alpha, \beta \end{matrix}\right] d\gamma_2. \end{aligned} \tag{6}$$

Now, by using the Meijer's *G* function representation of $\exp(-(m\gamma C/\Omega\gamma_2))$ as $\mathrm{G}_{0,1}^{1,0}\left[\frac{m\gamma C}{\Omega\gamma_2} \middle| \begin{matrix} - \\ 0 \end{matrix}\right]$ [30, Eq. (01.03.26.0004.01)] and the identity [31, Eq. (6.2.2)] to invert the argument in the Meijer's *G* function as $\mathrm{G}_{0,1}^{1,0}\left[\frac{m\gamma C}{\Omega\gamma_2} \middle| \begin{matrix} - \\ 0 \end{matrix}\right] = \mathrm{G}_{1,0}^{0,1}\left[\frac{\Omega\gamma_2}{m\gamma C} \middle| \begin{matrix} 1 \\ - \end{matrix}\right]$, the CDF of γ can be shown to be given by

$$\begin{aligned} F_\gamma(\gamma) = 1 - \frac{\xi^2(m-1)!\exp\left(-\frac{m\gamma}{\Omega}\right)}{r\Gamma(\alpha)\Gamma(\beta)\Gamma(m)} \sum_{k=0}^{m-1}\frac{1}{k!}\left(\frac{m\gamma}{\Omega}\right)^k \sum_{j=0}^{k}\binom{k}{j}C^j \\ \times \int_0^\infty \gamma_2^{-j-1}\mathrm{G}_{1,0}^{0,1}\left[\frac{\Omega\gamma_2}{m\gamma C} \middle| \begin{matrix} 1 \\ - \end{matrix}\right]\mathrm{G}_{1,3}^{3,0}\left[h\alpha\beta\left(\frac{\gamma_2}{\mu_r}\right)^{\frac{1}{r}} \middle| \begin{matrix} \xi^2 + 1 \\ \xi^2, \alpha, \beta \end{matrix}\right] d\gamma_2. \end{aligned} \tag{7}$$

Finally, along with the above modifications, we apply [32, Eq. (2.24.1.1)] and some mathematical manipulations to get the CDF of γ as

$$F_\gamma(\gamma) = 1 - A\exp\left(-\frac{m\gamma}{\Omega}\right)\sum_{k=0}^{m-1}\sum_{j=0}^{k}\frac{1}{j!(k-j)!}\left(\frac{m\gamma}{\Omega}\right)^{k-j}\mathrm{G}_{r,3r+1}^{3r+1,0}\left[\frac{BmC\gamma}{\mu_r\Omega} \middle| \begin{matrix} \kappa_1 \\ \kappa_2 \end{matrix}\right] \tag{8}$$

where $A = r^{\alpha+\beta-2}\xi^2/(2\pi)^{r-1}\Gamma(\alpha)\Gamma(\beta)$, $B = (h\,\alpha\,\beta)^r/r^{2r}$, $\kappa_1 = (\xi^2+1)/r,\ldots,(\xi^2+r)/r$ comprises r terms, and $\kappa_2 = \xi^2/r,\ldots,(\xi^2+r-1)/r,\alpha/r,\ldots,(\alpha+r-1)/r,\beta/r,\ldots,(\beta+r-1)/r,j$ comprises $3r+1$ terms. For $m=1$, as a special case, the CDF in (8) is in agreement with the CDF of the hybrid Rayleigh/FSO fixed gain dual hop transmission systems with pointing errors presented in [17, Eq. (2)]. The arguments of the Meijer's G function in (8) can be inverted using [31, Eq. (6.2.2)]. Then, by applying [29, Eq. (26)], the asymptotic expression of the CDF at **high SNR** can be derived in terms of basic elementary functions as

$$F_\gamma(\gamma) \underset{\mu_r\gg 1}{\approx} 1 - A\exp\left(-\frac{m\gamma}{\Omega}\right)\sum_{k=0}^{m-1}\sum_{j=0}^{k}\frac{1}{j!(k-j)!}\left(\frac{m\gamma}{\Omega}\right)^{k-j}\sum_{i=1}^{3r+1}\left(\frac{\Omega\mu_r}{BmC\gamma}\right)^{-\kappa_{2,i}}\frac{\prod_{l=1;l\neq i}^{3r+1}\Gamma(\kappa_{2,l}-\kappa_{2,i})}{\prod_{l=1}^{r}\Gamma(\kappa_{1,l}-\kappa_{2,i})} \quad (9)$$

where $\kappa_{u,v}$ stands for the vth-term of κ_u. This asymptotic expression for the CDF in (9) can be further expressed via only one dominant term j that represents the $(3r+1)$th-term in κ_2.

2.2.2. Probability Density Function

The PDF of γ can be obtained by differentiating (8) with respect to γ. Therefore, by applying [30, Eq. (07.34.20.0001.01)], we get the derivative of $\mathrm{G}_{r,3r+1}^{3r+1,0}\left[\frac{BmC\gamma}{\mu_r\Omega}\middle|\begin{matrix}\kappa_1\\ \kappa_2\end{matrix}\right]$ with respect to γ as $(BmC/\mu_r\Omega)\mathrm{G}_{r+1,3r+2}^{3r+1,1}\left[\frac{BmC\gamma}{\mu_r\Omega}\middle|\begin{matrix}-1,\kappa_1-1\\ \kappa_2-1,0\end{matrix}\right]$ that can be transformed into $(1/\gamma)\mathrm{G}_{r+1,3r+2}^{3r+1,1}\left[\frac{BmC\gamma}{\mu_r\Omega}\middle|\begin{matrix}0,\kappa_1\\ \kappa_2,1\end{matrix}\right]$ [30, Eq. (07.34.16.0001.01)]. Then, the PDF of γ can be obtained in exact closed-form in terms of the Meijer's G functions as

$$\begin{aligned} f_\gamma(\gamma) = A\exp\left(-\frac{m\gamma}{\Omega}\right)\Bigg\{&\frac{m}{\Omega}\sum_{k=0}^{m-1}\sum_{j=0}^{k}\frac{1}{j!(k-j)!}\left(\frac{m\gamma}{\Omega}\right)^{k-j}\mathrm{G}_{r,3r+1}^{3r+1,0}\left[\frac{BmC\gamma}{\mu_r\Omega}\middle|\begin{matrix}\kappa_1\\ \kappa_2\end{matrix}\right]\\ &-\sum_{k=0}^{m-1}\sum_{j=0}^{k}\frac{k-j}{j!(k-j)!}\frac{m}{\Omega}\left(\frac{m\gamma}{\Omega}\right)^{k-j-1}\mathrm{G}_{r,3r+1}^{3r+1,0}\left[\frac{BmC\gamma}{\mu_r\Omega}\middle|\begin{matrix}\kappa_1\\ \kappa_2\end{matrix}\right]\\ &-\sum_{k=0}^{m-1}\sum_{j=0}^{k}\frac{1}{j!(k-j)!}\left(\frac{m\gamma}{\Omega}\right)^{k-j}\frac{1}{\gamma}\mathrm{G}_{r+1,3r+2}^{3r+1,1}\left[\frac{BmC\gamma}{\mu_r\Omega}\middle|\begin{matrix}0,\kappa_1\\ \kappa_2,1\end{matrix}\right]\Bigg\}. \end{aligned} \quad (10)$$

The expression in (10) can be further simplified yielding

$$\begin{aligned} f_\gamma(\gamma) = A\exp\left(-\frac{m\gamma}{\Omega}\right)&\sum_{k=0}^{m-1}\sum_{j=0}^{k}\frac{1}{j!(k-j)!}\left(\frac{m\gamma}{\Omega}\right)^{k-j}\\ &\times\left\{\left(\frac{m}{\Omega}-\frac{k-j}{\gamma}\right)\mathrm{G}_{r,3r+1}^{3r+1,0}\left[\frac{BmC\gamma}{\mu_r\Omega}\middle|\begin{matrix}\kappa_1\\ \kappa_2\end{matrix}\right]\frac{1}{\gamma}\mathrm{G}_{r+1,3r+2}^{3r+1,1}\left[\frac{BmC\gamma}{\mu_r\Omega}\middle|\begin{matrix}0,\kappa_1\\ \kappa_2,1\end{matrix}\right]\right\}. \end{aligned} \quad (11)$$

For $m=1$, as a special case, the PDF in (11) is in a perfect agreement with the PDF in [17, Eq. (3)].

2.2.3. Moment Generating Function

It is well known that the MGF is defined as $\mathcal{M}_\gamma(s) = \mathbb{E}[e^{-\gamma s}]$. Using integration by parts, the MGF can be expressed in terms of the CDF as

$$\mathcal{M}_\gamma(s) = s\int_0^\infty e^{-\gamma s}F_\gamma(\gamma)d\gamma. \quad (12)$$

Placing (8) into (12), the MGF of γ can be formulated as

$$\mathcal{M}_\gamma(s) = s\int_0^\infty \exp(-\gamma s)d\gamma - sA\sum_{k=0}^{m-1}\sum_{j=0}^{k}\frac{\left(\frac{m}{\Omega}\right)^{k-j}}{j!(k-j)!}\int_0^\infty \gamma^{k-j}\exp\left(-\left(s+\frac{m}{\Omega}\right)\gamma\right)\mathrm{G}_{r,3r+1}^{3r+1,0}\left[\frac{BmC\gamma}{\mu_r\Omega}\middle|\begin{matrix}\kappa_1\\ \kappa_2\end{matrix}\right]d\gamma$$
$$= 1 - sA\sum_{k=0}^{m-1}\sum_{j=0}^{k}\frac{\left(\frac{m}{\Omega}\right)^{k-j}}{j!(k-j)!}\int_0^\infty \gamma^{k-j}\exp\left(-\left(s+\frac{m}{\Omega}\right)\gamma\right)\mathrm{G}_{r,3r+1}^{3r+1,0}\left[\frac{BmC\gamma}{\mu_r\Omega}\middle|\begin{matrix}\kappa_1\\ \kappa_2\end{matrix}\right]d\gamma. \quad (13)$$

Utilizing [30, Eq. (07.34.21.0088.01)] to solve the integral in (13), the MGF of γ can be presented in closed-form in terms of the Meijer's *G* function as

$$\mathcal{M}_\gamma(s) = 1 - sA\sum_{k=0}^{m-1}\sum_{j=0}^{k}\frac{\left(\frac{m}{\Omega}\right)^{k-j}}{j!(k-j)!}\left(s+\frac{m}{\Omega}\right)^{j-k-1}\mathrm{G}_{r+1,3r+1}^{3r+1,1}\left[\frac{BmC}{\mu_r(\Omega s+m)}\middle|\begin{matrix}j-k,\kappa_1\\ \kappa_2\end{matrix}\right]. \quad (14)$$

When $m = 1$, as a special case, the MGF in (14) can be easily shown to be equal to [17, Eq. (6)]. Similar to the CDF, the asymptotic expansion of the MGF at **high SNR** can be determined as

$$\mathcal{M}_\gamma(s) \underset{\mu_r\gg 1}{\approx} 1 - sA\sum_{k=0}^{m-1}\sum_{j=0}^{k}\frac{\left(\frac{m}{\Omega}\right)^{k-j}}{j!(k-j)!}\left(s+\frac{m}{\Omega}\right)^{j-k-1}$$
$$\times\sum_{i=1}^{3r+1}\left(\frac{\mu_r(\Omega s+m)}{BmC}\right)^{-\kappa_{2,i}}\frac{\prod_{l=1;l\neq i}^{3r+1}\Gamma(\kappa_{2,l}-\kappa_{2,i})\Gamma(1+\kappa_{2,i}-j+k)}{\prod_{l=1}^{r}\Gamma(\kappa_{1,l}-\kappa_{2,i})} \quad (15)$$

and can be further expressed via only the dominant term, j, which is the $(3r+1)^{\text{th}}$-term in κ_2.

2.2.4. Moments

The moments are specified as $\mathbb{E}[\gamma^n] = \int_0^\infty \gamma^n f_\gamma(\gamma)d\gamma$. Let $u = \gamma^n$ and $v = F_\gamma(\gamma)$. Using integration by parts, the moments can be expressed as

$$\mathbb{E}[\gamma^n] = n\int_0^\infty \gamma^{n-1}d\gamma - \int_0^\infty n\gamma^{n-1}F_\gamma(\gamma)d\gamma = n\int_0^\infty \gamma^{n-1}F_\gamma^c(\gamma)d\gamma \quad (16)$$

where $F_\gamma^c(\gamma) = 1 - F_\gamma(\gamma)$ is the complementary CDF (CCDF). Substituting (8) into (16), the moments can be rewritten as

$$\mathbb{E}[\gamma^n] = nA\sum_{k=0}^{m-1}\sum_{j=0}^{k}\frac{1}{j!(k-j)!}\left(\frac{m}{\Omega}\right)^{k-j}\int_0^\infty \gamma^{k-j+n-1}\exp\left(-\frac{m\gamma}{\Omega}\right)\mathrm{G}_{r,3r+1}^{3r+1,0}\left[\frac{BmC\gamma}{\mu_r\Omega}\middle|\begin{matrix}\kappa_1\\ \kappa_2\end{matrix}\right]. \quad (17)$$

Applying the integral identity [30, Eq. (07.34.21.0088.01)], the moments reduce to

$$\mathbb{E}[\gamma^n] = nA\left(\frac{\Omega}{m}\right)^n\sum_{k=0}^{m-1}\sum_{j=0}^{k}\frac{1}{j!(k-j)!}\mathrm{G}_{r+1,3r+1}^{3r+1,1}\left[\frac{BC}{\mu_r}\middle|\begin{matrix}1-k+j-n,\kappa_1\\ \kappa_2\end{matrix}\right]. \quad (18)$$

For $m=1$, as a special case, the moments in (18) can be easily shown to agree with [17, Eq. (8)]. It is important to mention that the moments are exploited to derive the expressions of the higher-order amount of fading in the next section.

2.3. Applications to the Performance of Asymmetric Nakagami-m/Unified FSO Relay Transmission Systems With Fixed Gain Relay

2.3.1. Outage Probability

The OP is an important measure for the performance of a wireless communication system. An outage of the communication system is encountered when the instantaneous output SNR γ

falls below a predetermined threshold γ_{th}. Setting $\gamma = \gamma_{th}$ in (8), we obtain the OP as

$$P_{out}(\gamma_{th}) = F_{\gamma}(\gamma_{th}). \tag{19}$$

2.3.2. Higher-Order Amount of Fading

For the instantaneous SNR γ, the n^{th}-order amount of fading is defined as [33]

$$AF_{\gamma}^{(n)} = \frac{\mathbb{E}[\gamma^n]}{\mathbb{E}[\gamma]^n} - 1. \tag{20}$$

Substituting (18) in (20) yields to the n^{th}-order AF.

2.3.3. Average BER

The average BER for a variety of binary modulations is introduced as [34, Eq. (12)]

$$\overline{P_b} = q^p 2\Gamma(p) \int_0^{\infty} \exp(-q\gamma)\gamma^{p-1} F_{\gamma}(\gamma) d\gamma \tag{21}$$

where p and q are parameters that change for different modulation schemes [35]. Substituting (8) into (21), the average BER can be expressed as

$$\overline{P_b} = \frac{q^p}{2\Gamma(p)} \mathcal{I}_1 - \frac{Aq^p}{2\Gamma(p)} \sum_{k=0}^{m-1} \sum_{j=0}^{k} \frac{\binom{m}{\Omega}^{k-j}}{j!(k-j)!} \mathcal{I}_2 \tag{22}$$

with $\mathcal{I}_1 = \int_0^{\infty} \gamma^{p-1} \exp(-q\gamma) d\gamma = q^{-p}\Gamma(p)$, and $\mathcal{I}_2$ can be derived utilizing [30, Eq. (07.34.21. 0088.01)] as

$$\begin{aligned} \mathcal{I}_2 &= \int_0^{\infty} \gamma^{p+k-j-1} \exp\left(-\left(q + \frac{m}{\Omega}\right)\gamma\right) \mathrm{G}_{r,3r+1}^{3r+1,0}\left[\frac{BmC\gamma}{\mu_r \Omega} \middle| \begin{matrix} \kappa_1 \\ \kappa_2 \end{matrix}\right] d\gamma \\ &= \left(q + \frac{m}{\Omega}\right)^{j-k-p} \mathrm{G}_{r+1,3r+1}^{3r+1,1}\left[\frac{BmC}{\mu_r(q\Omega + m)} \middle| \begin{matrix} 1-p-k+j, \kappa_1 \\ \kappa_2 \end{matrix}\right]. \end{aligned} \tag{23}$$

Finally, we obtain the BER as

$$\overline{P_b} = \frac{1}{2} - \frac{Aq^p}{2\Gamma(p)} \sum_{k=0}^{m-1} \sum_{j=0}^{k} \frac{\binom{m}{\Omega}^{k-j}}{j!(k-j)!} \left(q + \frac{m}{\Omega}\right)^{j-k-p} \mathrm{G}_{r+1,3r+1}^{3r+1,1}\left[\frac{BmC}{\mu_r(q\Omega + m)} \middle| \begin{matrix} 1-p-k+j, \kappa_1 \\ \kappa_2 \end{matrix}\right]. \tag{24}$$

For $m = 1$, as a special case, we get the BER of the mixed Rayleigh-FSO fixed gain dual hop transmission systems with pointing errors given in [17, Eq. (11)]. At **high SNR** and similar to the CDF, the BER can be expressed asymptotically as

$$\begin{aligned} \overline{P_b} \underset{\mu_r \gg 1}{\approx} \frac{1}{2} - \frac{Aq^p}{2\Gamma(p)} \sum_{k=0}^{m-1} \sum_{j=0}^{k} \frac{\binom{m}{\Omega}^{k-j}}{j!(k-j)!} \left(q + \frac{m}{\Omega}\right)^{j-k-p} \\ \times \sum_{i=1}^{3r+1} \left(\frac{\mu_r(q\Omega + m)}{BmC}\right)^{-\kappa_{2,i}} \frac{\prod_{l=1; l\neq i}^{3r+1} \Gamma(\kappa_{2,l} - \kappa_{2,i}) \Gamma(\kappa_{2,i} + p + k - j)}{\prod_{l=1}^{r} \Gamma(\kappa_{1,l} - \kappa_{2,i})} \end{aligned} \tag{25}$$

and can be further expressed via only the dominant term j.

2.3.4. Ergodic Capacity

The ergodic capacity defined as $\overline{C} = \mathbb{E}[\log_2(1 + c\gamma)]$, where $c = 1$ for heterodyne detection and $c = e/(2\pi)$ for IM/DD [36, Eq. (26)], [37, Eq. (7.43)], can be written in terms of the CCDF of

γ as [38, Eq. (15)]

$$\overline{C} = 1/\ln(2) \int_0^{\infty} F_{\gamma}^{c}(\gamma)/(1+c\gamma)d\gamma. \tag{26}$$

Using [39] to represent $(1+c\gamma)^{-1}$ as $\mathrm{G}_{1,1}^{1,1}\left[c\gamma \middle| \begin{matrix} 0 \\ 0 \end{matrix}\right]$, and utilizing the integral identity [34, Eq. (20)], we obtain the ergodic capacity in terms of the EGBMGF as

$$\overline{C} = \frac{A}{\ln(2)} \frac{\Omega}{m} \sum_{k=0}^{m-1} \sum_{j=0}^{k} \frac{1}{j!(k-j)!} \mathrm{G}_{1,0:1,1:r,3r+1}^{1,0:1,1:3r+1,0}\left[k-j+1 \middle| \begin{matrix} 0 \\ 0 \end{matrix} \middle| \begin{matrix} \kappa_1 \\ \kappa_2 \end{matrix} \middle| \frac{\Omega}{m}, \frac{BC}{c\mu_r}\right]. \tag{27}$$

An efficient MATHEMATICA implementation of the EGBMGF is given in [34, Table II]. It is noteworthy that in the case of IM/DD technique, the ergodic capacity is lower bounded by (27) whereas for the heterodyne detection technique, the formula derived in (27) acts as an exact expression for the system ergodic capacity. For $m = 1$, as a special case, the ergodic capacity in (27) is in agreement with [17, Eq. (13)].

3. Asymmetric Nakagami-*m*/Unified FSO Relay Transmission Systems With Variable Gain Relay

3.1. Channel and System Models

We employ the same model as is described in the previous section except that we are considering variable gain relay. Hence, the end-to-end SNR can be given as

$$\gamma = \frac{\gamma_1 \gamma_2}{\gamma_1 + \gamma_2 + 1}. \tag{28}$$

The closed-form analytical derivation of the SNR statistics in (28) is mathematically intractable. Therefore, we approximate the end-to-end SNR γ as [40]

$$\gamma = \frac{\gamma_1 \gamma_2}{\gamma_1 + \gamma_2 + 1} \cong \min(\gamma_1, \gamma_2). \tag{29}$$

3.2. Statistical Characteristics

3.2.1. Cumulative Distribution Function

The CDF of $\gamma = \min(\gamma_1, \gamma_2)$ can be expressed as

$$F_{\gamma}(\gamma) = \Pr(\min(\gamma_1, \gamma_2) < \gamma), \tag{30}$$

which can be rewritten as [41, Eq. (4)]

$$F_{\gamma}(\gamma) = F_{\gamma_1}(\gamma_1) + F_{\gamma_2}(\gamma_2) - F_{\gamma_1}(\gamma_1) F_{\gamma_2}(\gamma_2), \tag{31}$$

where $F_{\gamma_1}(\gamma_1)$ and $F_{\gamma_2}(\gamma_2)$ are the CDFs of γ_1 and γ_2, respectively. We can express the CDF of the RF S–R link $F_{\gamma_1}(\gamma_1)$ as

$$F_{\gamma_1}(\gamma_1) = \int_0^{\gamma_1} f_{\gamma_1}(t)dt = 1 - \frac{1}{\Gamma(m)} \Gamma\left(m, \frac{m\gamma_1}{\Omega}\right). \tag{32}$$

The CDF of the FSO R–D link $F_{\gamma_2}(\gamma_2)$ is given in [29, Eq. (5)] as

$$F_{\gamma_2}(\gamma_2) = A\, \mathrm{G}_{r+1,3r+1}^{3r,1}\left[\frac{B}{\mu_r}\gamma_2 \middle| \begin{matrix} 1, \kappa_1 \\ \kappa_2, 0 \end{matrix}\right]. \tag{33}$$

After some algebraic manipulations and simplifications, the CDF of γ can be found as

$$F_\gamma(\gamma) = 1 + \frac{\Gamma\left(m, \frac{m\gamma}{\Omega}\right)}{\Gamma(m)} \left[A\, \mathrm{G}_{r+1,3r+1}^{3r,1} \left[\frac{B\gamma}{\mu_r} \middle| \begin{matrix} 1, \kappa_1 \\ \kappa_2, 0 \end{matrix} \right] - 1 \right]. \tag{34}$$

It is noteworthy that the above expression is valid for both integer and non integer m's. For $m = 1$, as a special case, we obtain the BER of the mixed Rayleigh-FSO variable gain dual-hop transmission systems with pointing errors given in [18, Eq. (5)]. Moreover, the CDF can be expressed asymptotically by using the Meijer's G function expansion given in [29, Eq. (26)], at **high SNR**, as

$$F_\gamma(\gamma) \underset{\mu_r \gg 1}{\approx} 1 + \frac{\Gamma\left(m, \frac{m\gamma}{\Omega}\right)}{\Gamma(m)} \left\{ A \sum_{i=1}^{3r} \left(\frac{\mu_r}{B\gamma} \right)^{-\kappa_{2,i}} \frac{\prod_{l=1; l\neq i}^{3r} \Gamma(\kappa_{2,l} - \kappa_{2,i})}{\kappa_{2,i} \prod_{l=1}^{r} \Gamma(\kappa_{1,l} - \kappa_{2,i})} - 1 \right\}. \tag{35}$$

The asymptotic expression for the CDF in (35) is dominated by $\min(\xi^2/r, \alpha/r, \beta/r)$ where ξ^2/r accounts for the 1st-term, α/r stands for the $(r+1)$th-term, and β/r represents the $(2r+1)$th-term in κ_2.

3.2.2. Probability Density Function

Taking the derivative of $F_\gamma(\gamma)$ with respect to γ, using [30, Eq. (07.34.20.0001.01)] to get the derivative of $\mathrm{G}_{r+1,3r+1}^{3r,1}\left[B\gamma/\mu_r \middle| \begin{matrix} 1, \kappa_1 \\ \kappa_2, 0 \end{matrix} \right]$ as $(B/\mu_r)\mathrm{G}_{r+2,3r+2}^{3r,2}\left[\frac{B\gamma}{\mu_r} \middle| \begin{matrix} -1, 0, \kappa_1 - 1 \\ \kappa_2 - 1, 0, -1 \end{matrix} \right]$, and using [30, Eq. (06.06.20.0003.01)] to obtain the derivative of $\Gamma(m, (m\gamma/\Omega))$ as $-(m/\Omega) \times \exp(-(m\gamma/\Omega))(m\gamma/\Omega)^{m-1}$ then applying the product rule, the PDF can be expressed as

$$\begin{aligned} f_\gamma(\gamma) = {} & \frac{m}{\Omega\Gamma(m)} \exp\left(-\frac{m\gamma}{\Omega}\right) \left(\frac{m\gamma}{\Omega}\right)^{m-1} - \frac{mA}{\Omega\Gamma(m)} \exp\left(-\frac{m\gamma}{\Omega}\right) \left(\frac{m\gamma}{\Omega}\right)^{m-1} \mathrm{G}_{r+1,3r+1}^{3r,1} \left[\frac{B\gamma}{\mu_r} \middle| \begin{matrix} 1, \kappa_1 \\ \kappa_2, 0 \end{matrix} \right] \\ & + \frac{AB}{\mu_r \Gamma(m)} \Gamma\left(m, \frac{m\gamma}{\Omega}\right) \mathrm{G}_{r+2,3r+2}^{3r,2} \left[\frac{B\gamma}{\mu_r} \middle| \begin{matrix} 1, 0, \kappa_1 - 1 \\ \kappa_2 - 1, 0, -1 \end{matrix} \right]. \end{aligned} \tag{36}$$

By applying [30, Eq. (07.34.16.0001.01)], we can transform $(B/\mu_r)\mathrm{G}_{r+2,3r+2}^{3r,2}\left[\frac{B\gamma}{\mu_r} \middle| \begin{matrix} -1, 0, \kappa_1 - 1 \\ \kappa_2 - 1, 0, -1 \end{matrix} \right]$ into $(1/\gamma)\mathrm{G}_{r+2,3r+2}^{3r,2}\left[\frac{B\gamma}{\mu_r} \middle| \begin{matrix} 0, 1, \kappa_1 \\ \kappa_2, 1, 0 \end{matrix} \right]$. Eventually, the expression in (36) becomes

$$\begin{aligned} f_\gamma(\gamma) = {} & -\frac{\gamma^{m-1}}{\Gamma(m)} \left(\frac{m}{\Omega}\right)^m \exp\left(-\frac{m\gamma}{\Omega}\right) \left\{ -1 + A\, \mathrm{G}_{r+1,3r+1}^{3r,1} \left[\frac{B\gamma}{\mu_r} \middle| \begin{matrix} 1, \kappa_1 \\ \kappa_2, 0 \end{matrix} \right] \right\} \\ & + \frac{A}{\Gamma(m)} \frac{1}{\gamma} \Gamma\left(m, \frac{m\gamma}{\Omega}\right) \mathrm{G}_{r+2,3r+2}^{3r,2} \left[\frac{B\gamma}{\mu_r} \middle| \begin{matrix} 0, 1, \kappa_1 \\ \kappa_2, 1, 0 \end{matrix} \right]. \end{aligned} \tag{37}$$

The expression in (37) can be applied for both integer and non integer values of m. For $m = 1$, as a special case, the PDF in (37) is in agreement with [18, Eq. (6)].

3.2.3. Moment Generating Function

Substituting (34) in (12), the MGF of γ can be given by

$$\begin{aligned} \mathcal{M}_\gamma(s) = {} & s \int_0^\infty \exp(-\gamma s) d\gamma - \frac{s}{\Gamma(m)} \int_0^\infty e^{-\gamma s} \Gamma\left(m, \frac{m\gamma}{\Omega}\right) d\gamma \\ & + \frac{sA}{\Gamma(m)} \int_0^\infty \exp(-\gamma s) \Gamma\left(m, \frac{m\gamma}{\Omega}\right) \mathrm{G}_{r+1,3r+1}^{3r,1} \left[\frac{B\gamma}{\mu_r} \middle| \begin{matrix} 1, \kappa_1 \\ \kappa_2, 0 \end{matrix} \right] d\gamma. \end{aligned} \tag{38}$$

Utilizing the identity [28, Eq. (6.451.2)] with the change of variable $z = (m\gamma)/\Omega$, we get $\int_0^\infty \exp(-\gamma s)\Gamma(m,(m\gamma/\Omega))d\gamma = (\Gamma(m)/s)[1-(1+(s\Omega/m))^{-m}]$. Then, exploiting [30, Eq. (06.06.26.0005.01)] to represent $\Gamma(m,(m\gamma/\Omega))$ as $\mathrm{G}_{1,2}^{2,0}\left[\frac{m\gamma}{\Omega}\middle| \begin{matrix}1\\0,m\end{matrix}\right]$, and using [30, Eq. (01.03.26.0004.01)] to rewrite $\exp(-\gamma s)$ as $\mathrm{G}_{1,0}^{0,1}\left[\gamma s\middle| \begin{matrix}-\\0\end{matrix}\right]$, the MGF in (38) can be expressed as

$$\mathcal{M}_\gamma(s) = \left(1+\frac{s\Omega}{m}\right)^{-m} + \frac{sA}{\Gamma(m)}\int_0^\infty \mathrm{G}_{0,1}^{1,0}\left[\gamma s\middle| \begin{matrix}-\\0\end{matrix}\right]\mathrm{G}_{1,2}^{2,0}\left[\frac{m\gamma}{\Omega}\middle| \begin{matrix}1\\0,m\end{matrix}\right]\mathrm{G}_{r+1,3r+1}^{3r,1}\left[\frac{B\gamma}{\mu_r}\middle| \begin{matrix}1,\kappa_1\\\kappa_2,0\end{matrix}\right]d\gamma. \tag{39}$$

Finally, we apply the integral identity [42, Eq. (12)] to obtain the MGF of γ in terms of the EGBMGF function as

$$\mathcal{M}_\gamma(s) = \left(1+\frac{s\Omega}{m}\right)^{-m} + \frac{s\Omega A}{m\Gamma(m)}\mathrm{G}_{2,1:0,1:r+1,3r+1}^{2,0:1,0:3r,1}\left[\begin{matrix}1,m+1\\2\end{matrix}\middle| \begin{matrix}-\\0\end{matrix}\middle| \begin{matrix}1,\kappa_1\\\kappa_2,0\end{matrix}\middle| \frac{s\Omega}{m},\frac{B\Omega}{\mu_r m}\right]. \tag{40}$$

Note that, the MGF in (40) is not restricted to integer values of *m*. Alternatively, utilizing [28, Eq. (8.352.7)] by expressing $\Gamma(m,(m\gamma/\Omega))$ as $(m-1)!\exp(-(m\gamma/\Omega)\sum_{k=0}^{m-1}(1/k!)(m\gamma/\Omega)^k$ for positive integer *m* then using the integral identity [30, Eq. (07.34.21.0088.01)], we obtain after further algebraic manipulations the MGF in exact closed-form result in terms of the Meijer's *G* function as

$$\mathcal{M}_\gamma(s) = \left(1+\frac{s\Omega}{m}\right)^{-m} + sA\sum_{k=0}^{m-1}\frac{\left(\frac{m}{\Omega}\right)^k}{k!}\left(s+\frac{m}{\Omega}\right)^{-k-1}\mathrm{G}_{r+2,3r+1}^{3r,2}\left[\frac{B}{\mu_r\left(s+\frac{m}{\Omega}\right)}\middle| \begin{matrix}-k,1,\kappa_1\\\kappa_2,0\end{matrix}\right]. \tag{41}$$

For $m=1$, as a special case, the MGF in (40) and (41) provides a perfect match to the MGF in [18, Eq. (8)]. Additionally, by exploiting the Meijer's G expansion [29, Eq. (26)] in (41), the asymptotic expression of the MGF can be given as

$$\begin{aligned}\mathcal{M}_\gamma(s) \underset{\mu_r\gg 1}{\approx} &\left(1+\frac{s\Omega}{m}\right)^{-m} + sA\sum_{k=0}^{m-1}\frac{\left(\frac{m}{\Omega}\right)^k}{k!}\times\left(s+\frac{m}{\Omega}\right)^{-k-1}\\ &\times\sum_{i=1}^{3r}\left(\frac{\left(s+\frac{m}{\Omega}\right)\mu_r}{B}\right)^{-\kappa_{2,i}}\frac{\prod_{l=1;l\neq i}^{3r}\Gamma(\kappa_{2,l}-\kappa_{2,i})\prod_{l=1}^{2}\Gamma(1+\kappa_{2,i}-\kappa_{1,l})}{\Gamma(1+\kappa_{2,i})\prod_{l=1}^{r}\Gamma(\kappa_{1,l}-\kappa_{2,i})}\end{aligned} \tag{42}$$

and can be further expressed via only the dominant term, $\min(\xi^2/r,\alpha/r,\beta/r)$.

3.2.4. Moments

Placing (34) into (16), using [30, Eq. (06.06.26.0005.01)] to transform $\Gamma(m,(m\gamma/\Omega))$ to $\mathrm{G}_{1,2}^{2,0}\left[\frac{m\gamma}{\Omega}\middle| \begin{matrix}1\\0,m\end{matrix}\right]$, and integrating utilizing [30, Eq. (07.34.21.0011.01)], the moments can be determined as

$$\mathbb{E}[\gamma^n] = \frac{1}{\Gamma(m)}\left(\frac{\Omega}{m}\right)^n\left\{\Gamma(m+n) - nA\,\mathrm{G}_{r+3,3r+2}^{3r,3}\left[\frac{B\Omega}{m\mu_r}\middle| \begin{matrix}1,1-n,1-n-m,\kappa_1\\\kappa_2,-n,0\end{matrix}\right]\right\}. \tag{43}$$

The closed-form expression given in (43) can be used with integer and non-integer values of *m*. For $m=1$, as a special case, we get the moments in [18, Eq. (10)].

3.3. Applications to the Performance of Asymmetric Nakagami-m/Unified FSO Relay Transmission Systems With Variable Gain Relay

3.3.1. Outage Probability

Similar to the OP of the fixed gain relay system derived earlier, the OP of the variable relay scheme can be derived from (34).

3.3.2. Higher-Order Amount of Fading

Substituting (43) into (20), we can derive the expression of the n^{th}-order amount of fading.

3.3.3. Average BER

Utilizing (21) by placing (34) into it, using the integral identity [28, Eq. (7.813.1)], representing the exponential and the incomplete Gamma functions through Meijer's *G* functions, and applying the integral identity [42, Eq. (12)], the BER can be shown to be given in terms of both the EGBMGF and the Meijer's *G* functions as

$$\overline{P_b} = \frac{1}{2} - \frac{1}{2\Gamma(p)\Gamma(m)} \mathrm{G}_{2,2}^{2,1}\left[\frac{m}{q\Omega}\middle| \begin{matrix} 1-p, 1 \\ 0, m \end{matrix}\right] + \frac{q^p \Omega A}{2m\Gamma(p)\Gamma(m)} \left(\frac{\mu_r}{B}\right)^{p-1} \times \mathrm{G}_{2,1:0,1:r+1,3r+1}^{2,0:1,0:3r,1}\left[\begin{matrix} 1, m+1 \\ 2 \end{matrix}\middle| \begin{matrix} - \\ 0 \end{matrix}\middle| \begin{matrix} p, \kappa_1 + p - 1 \\ \kappa_2 + p - 1, p - 1 \end{matrix}\middle| \frac{q\Omega}{m}, \frac{B\Omega}{\mu_r m}\right]. \quad (44)$$

Note that the average BER given in (44) is valid for any arbitrary m (i.e., integer and non integer). Similar to the MGF, writing $\Gamma(m,(m\gamma/\Omega))$ as $(m-1)!\exp(-(m\gamma/\Omega))\sum_{k=0}^{m-1}(1/k!)(m\gamma/\Omega)^k$ for positive integer m then using [28, Eq. (7.813.1)], we can get the average BER of a variety of binary modulations in exact closed-form in terms of Meijer's *G* functions only as

$$\overline{P_b} = \frac{1}{2} - \frac{1}{2\Gamma(p)\Gamma(m)} \mathrm{G}_{2,2}^{2,1}\left[\frac{m}{q\Omega}\middle| \begin{matrix} 1-p, 1 \\ 0, m \end{matrix}\right] + \frac{q^p A}{2\Gamma(p)} \times \sum_{k=0}^{m-1} \frac{\left(\frac{m}{\Omega}\right)^k}{k!} \left(q + \frac{m}{\Omega}\right)^{-k-p} \mathrm{G}_{r+2,3r+1}^{3r,2}\left[\frac{B}{\mu_r\left(q+\frac{m}{\Omega}\right)}\middle| \begin{matrix} 1-p-k, 1, \kappa_1 \\ \kappa_2, 0 \end{matrix}\right]. \quad (45)$$

For $m = 1$, as a special case, the BER in (45) coincide with the BER of the mixed RF/FSO variable gain dual-hop system in [18, Eq. (15)]. Moreover, we can derive an asymptotic expression for the BER at **high SNR** as

$$\overline{P_b} \underset{\mu_r \gg 1}{\approx} \frac{1}{2} - \frac{1}{2\Gamma(p)\Gamma(m)} \mathrm{G}_{2,2}^{2,1}\left[\frac{m}{q\Omega}\middle| \begin{matrix} 1-p, 1 \\ 0, m \end{matrix}\right] + \frac{q^p A}{2\Gamma(p)} \times \sum_{k=0}^{m-1} \frac{\left(\frac{m}{\Omega}\right)^k}{k!} \left(q + \frac{m}{\Omega}\right)^{-k-p} \times \sum_{i=1}^{3r} \left(\frac{\left(q+\frac{m}{\Omega}\right)\mu_r}{B}\right)^{-\kappa_{2,i}} \frac{\prod_{l=1;l\neq i}^{3r} \Gamma(\kappa_{2,l} - \kappa_{2,i}) \prod_{l=1}^{2} \Gamma(1 + \kappa_{2,i} - \kappa_{1,l})}{\Gamma(1+\kappa_{2,i}) \prod_{l=1}^{r} \Gamma(\kappa_{1,l} - \kappa_{2,i})}. \quad (46)$$

3.3.4. Ergodic Capacity

Similar to the previous section, on substituting (34) into (26), exploiting the identity in [39] to transform $(1+c\gamma)^{-1}$ into $\mathrm{G}_{1,1}^{1,1}\left[c\gamma\middle| \begin{matrix} 0 \\ 0 \end{matrix}\right]$, rewriting $\Gamma(m,(m\gamma/\Omega))$ as $\mathrm{G}_{1,2}^{2,0}\left[\frac{m\gamma}{\Omega}\middle| \begin{matrix} 1 \\ 0, m \end{matrix}\right]$, then using the integral identities [42, Eq. (12)] and [30, Eq. (07.34.21.0011.01)], the ergodic capacity can be derived in terms of the EGBMGF as

$$\overline{C} = \frac{1}{\Gamma(m)\ln(2)} \left\{ \mathrm{G}_{2,3}^{3,1}\left[\frac{m}{\Omega}\middle| \begin{matrix} 0, 1 \\ 0, m, 0 \end{matrix}\right] - \frac{\Omega A}{m} \mathrm{G}_{2,1:1,1:r+1,3r+1}^{2,0:1,1:3r,1}\left[\begin{matrix} 1, m+1 \\ 2 \end{matrix}\middle| \begin{matrix} 0 \\ 0 \end{matrix}\middle| \begin{matrix} 1, \kappa_1 \\ \kappa_2, 0 \end{matrix}\middle| \frac{\Omega}{m}, \frac{B\Omega}{mc\mu_r}\right] \right\}. \quad (47)$$

Similarly, the ergodic capacity expression derived in (47) can be utilized with both integer and non integer m's. It is noted that for $m = 1$, as a special case, the ergodic capacity in (47) simplifies to [18, Eq. (17)].

4. Numerical Results

In this section, we present simulation and numerical results for different performance metrics of asymmetric dual-hop Nakagami-*m*/unified FSO relay transmission systems with fixed

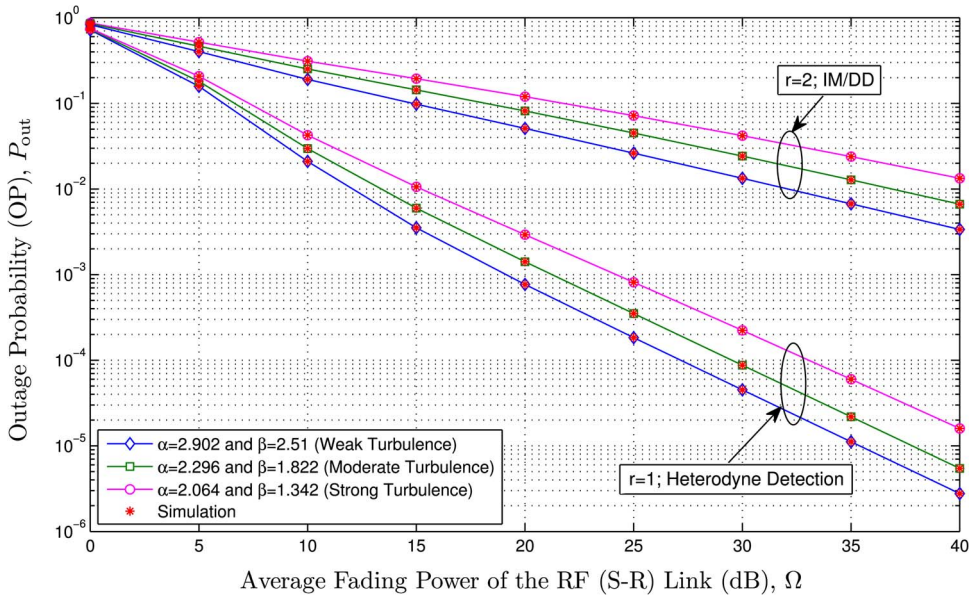

Fig. 2. OP showing the performance of both the detection techniques (heterodyne and IM/DD) under strong, moderate, and weak turbulent FSO channels for strong pointing error $\xi = 1.1$ for the fixed gain relay scheme.

and variable gains at the relay, as an illustration of the analytical expressions given in the previous sections. The FSO link (i.e., the R–D link) is modeled by a unified Gamma–Gamma fading channel for weak ($\alpha = 2.902$ and $\beta = 2.51$), moderate ($\alpha = 2.296$ and $\beta = 1.822$), and strong ($\alpha = 2.064$ and $\beta = 1.342$) turbulent FSO channel conditions [43, Table I].

4.1. Constant Gain Relay Scenario

In this section, the average SNR between the relay and the0 destination (R–D link) is set such that $\overline{\gamma}_2 = 10$ dB except for the figures showing the asymptotic results where $\overline{\gamma}_2$ is varying. For the fixed gain scheme, the relay is set such as $C = 1$.

The outage probability performance for both heterodyne and IM/DD detection techniques versus the normalized average fading power of the RF link (i.e., S–R link) is presented in Fig. 2. The effect of pointing error is fixed at $\xi = 1.1$. We can see from Fig. 2 that the analytical results provide a perfect match to the simulation results presented in this paper. It can also be observed that heterodyne detection technique $(r = 1)$, despite of its complexity, provides better performance than the IM/DD technique $(r = 2)$. Moreover, it can be shown that the performance deteriorates as the atmospheric turbulence conditions get severe (i.e., the higher the values of α and β, the lower will be the OP) and vice versa.

In Fig. 3, we illustrate the OP under IM/DD technique with varying effects of the pointing error ($\xi = 1$ and 6.7). As expected, the OP increases as the pointing error gets severe (i.e., the lower the values of ξ, the higher will be the OP). Additionally, it can be observed that for lower effect of the atmospheric turbulence, the respective performance gets better.

Fig. 4 demonstrates the average BER performance for differential binary phase shift keying (DBPSK) binary modulation scheme where $p = 1$ and $q = 1$ are the parameters of DBPSK, for both types of detection techniques (i.e., IM/DD and heterodyne detection) with fixed effect of the pointing error $(\xi = 1.1)$. As clearly seen in the figure, the analytical results and the simulation results coincide. We can also see from this figure that the heterodyne detection technique outperforms the IM/DD technique. Moreover, it can be observed that the performance improves as the effect of the atmospheric turbulence drops.

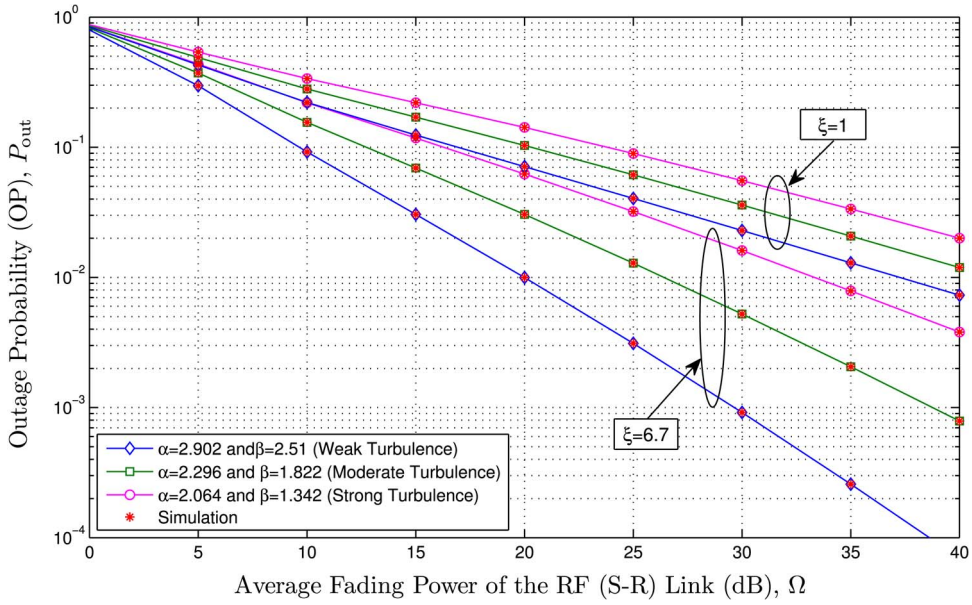

Fig. 3. OP showing the performance of IM/DD technique under strong, moderate, and weak turbulent FSO channels with varying effects of the pointing error for the fixed gain relay scheme.

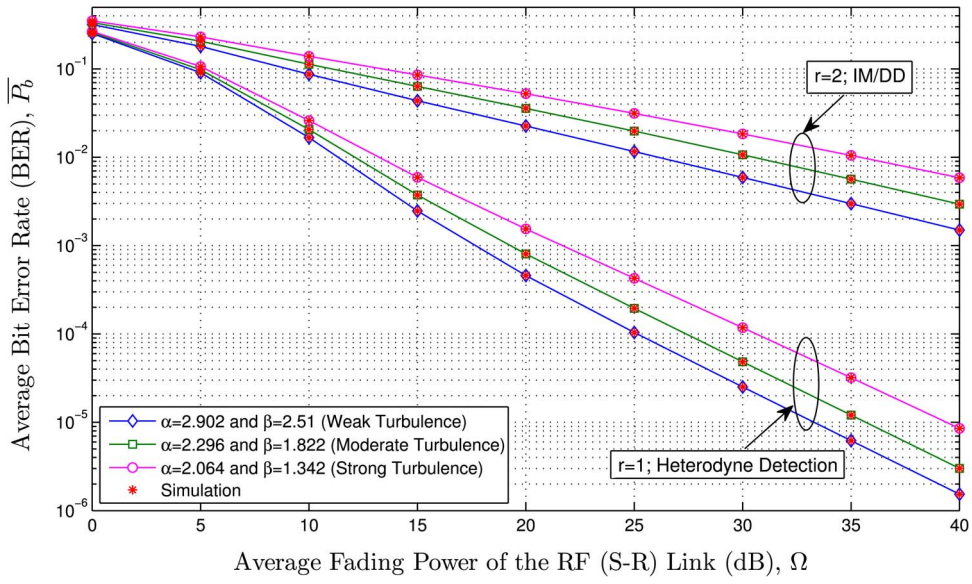

Fig. 4. Average BER of DBPSK binary modulation scheme showing the performance of both the detection techniques (heterodyne detection and IM/DD) under strong, moderate, and weak turbulent FSO channels for strong pointing error $\xi = 1.1$ for the fixed gain relay scheme.

Fig. 5 depicts the average BER for DBPSK binary modulation scheme under IM/DD technique for varying effects of the pointing error ($\xi = 1$ and 6.7). Expectedly, as the effect of the pointing error decreases ($\xi \to \infty$), the respective system performance gets better.

Fig. 6 presents the average BER for DBPSK binary modulation scheme under both heterodyne and IM/DD technique techniques for strong pointing error along with the asymptotic results at high SNR. It can be observed that at high SNR, the asymptotic expression utilizing the Meijer's *G* function expansion and considering all the terms in the summation in (25) converges to the exact result at high power regime of the FSO link proving the tightness of this

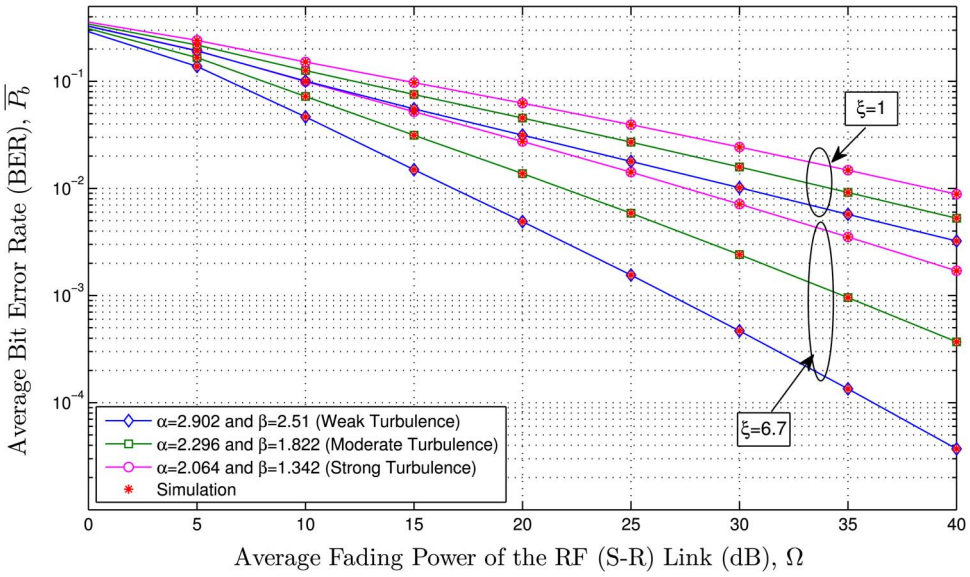

Fig. 5. Average BER of DBPSK binary modulation scheme showing the performance of IM/DD technique under strong, moderate, and weak turbulent FSO channels with varying effects of the pointing error for the fixed gain relay scheme.

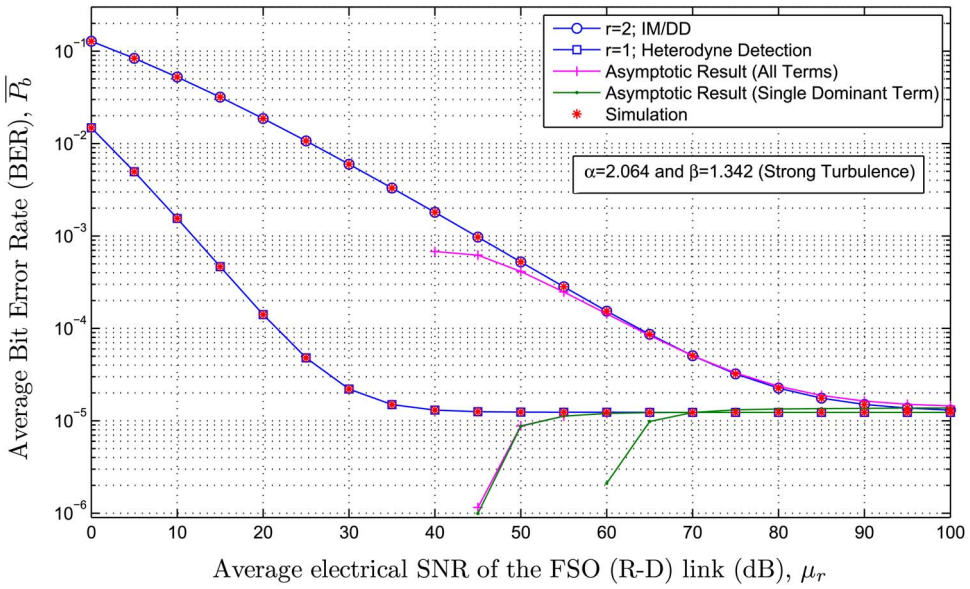

Fig. 6. Average BER of DBPSK binary modulation scheme showing the performance of both the detection techniques under strong turbulence conditions for strong pointing error $\xi = 1.1$ along with the asymptotic results at high SNR regime for $\Omega = 20$ dB for the fixed gain relay scheme.

asymptotic approximation. Additionally, when we select the relevant single dominant term of (25) derived via the Meijer's *G* function expansion in terms of simpler functions, a slower convergence is clearly observed, especially for the heterodyne detection technique.

In Fig. 7, the ergodic capacity under both heterodyne and IM/DD detection techniques for varying effects of the pointing error ($\xi = 1$ and 6.7) for strong turbulence conditions is presented. It can be observed that heterodyne detection performs much better than the IM/DD technique. Additionally, it can be shown that as the pointing error gets severe, the ergodic capacity decreases (i.e., the higher values of ξ, the higher will be the ergodic capacity).

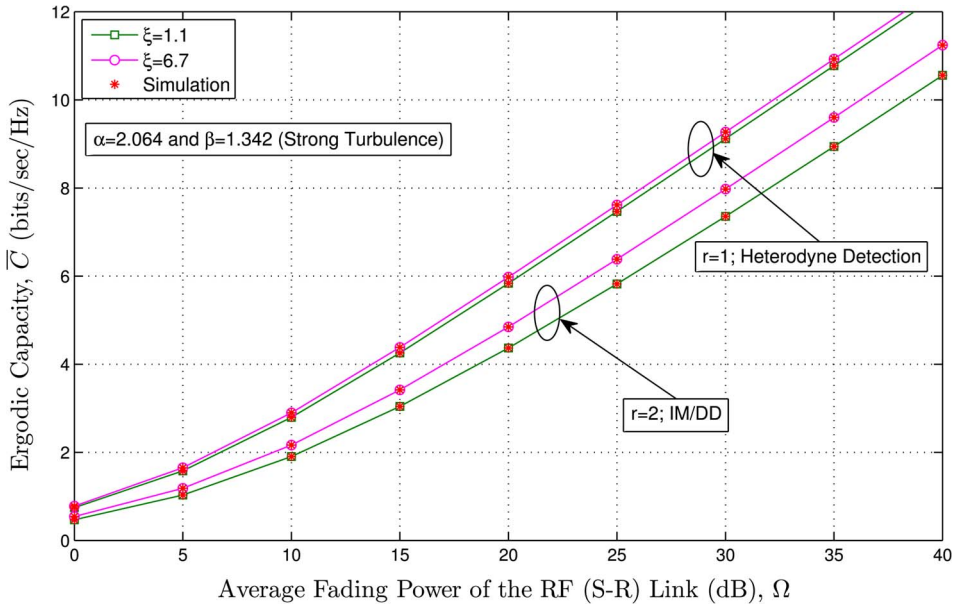

Fig. 7. Ergodic capacity results showing the performance of both heterodyne and IM/DD techniques under strong turbulence conditions for varying pointing errors for the fixed gain relay scheme.

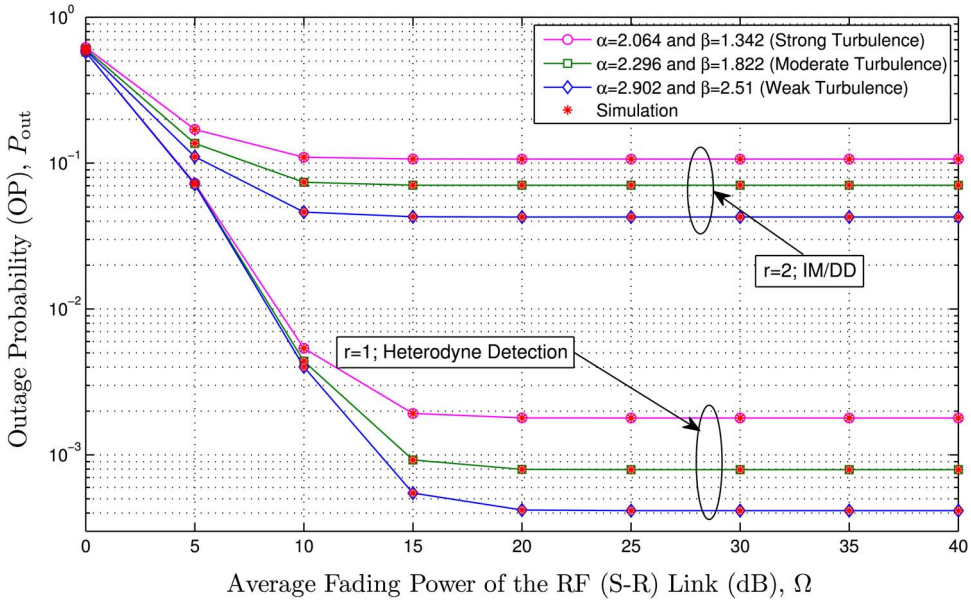

Fig. 8. OP showing the performance of both the detection techniques under strong, moderate, and weak turbulent FSO channels for strong pointing error $\xi = 1.1$ for the variable gain relay scheme.

4.2. Variable Gain Relay Scenario

In this section, the average SNR between the relay and the destination (R–D link) is set such as $\overline{\gamma}_2 = 30$ dB except for the figures showing the asymptotic results where $\overline{\gamma}_2$ is varying.

Fig. 8 presents the outage probability performance for both heterodyne and IM/DD detection techniques versus the normalized average fading power of the RF link (i.e., S–R link). The effect of pointing error is set such that $\xi = 1.1$. According to the figure, it is clearly seen that the analytical results are in a perfect agreement with the simulation results. It can also be seen that the heterodyne detection technique performs better than the IM/DD technique. Moreover, it can be

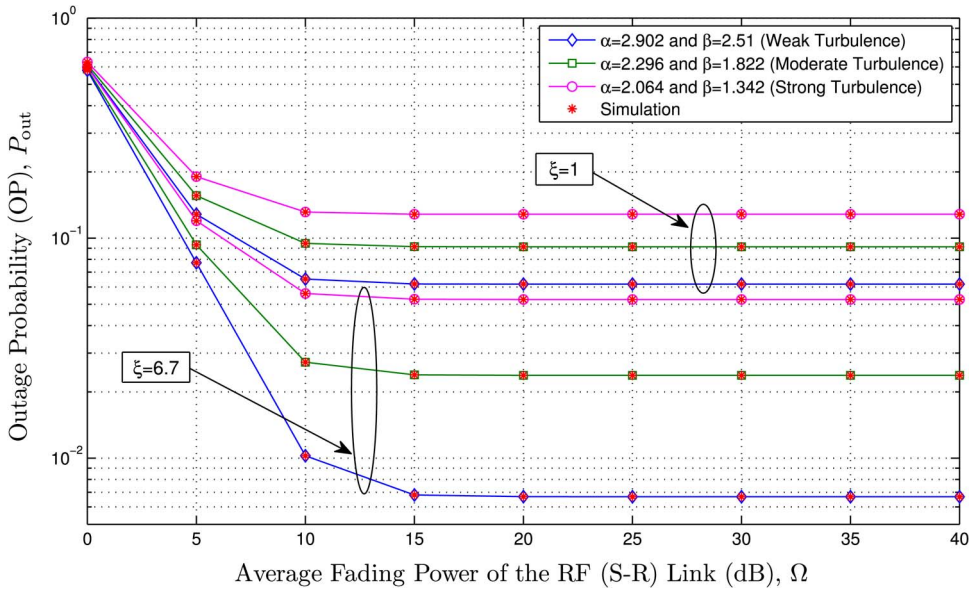

Fig. 9. OP showing the performance of the IM/DD technique under strong, moderate, and weak turbulent FSO channels with varying effects of the pointing error for the variable gain relay scheme.

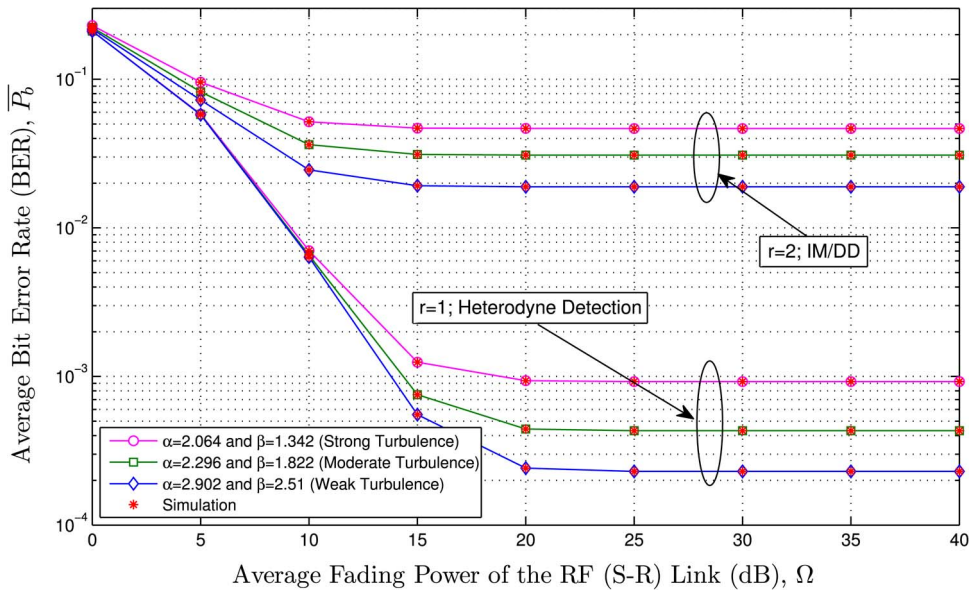

Fig. 10. Average BER of the DBPSK binary modulation scheme showing the performance of both the detection techniques (heterodyne and IM/DD) under strong, moderate, and weak turbulent FSO channels for strong pointing error $\xi = 1.1$ for the variable gain relay scheme.

observed that as the atmospheric turbulence conditions get severe, the OP increases. Finally, it can be clearly observed from Fig. 8 that when the average fading power Ω of the RF link (S–R link) becomes equal to the average SNR $\overline{\gamma}_2$ of the FSO link (R–D link) (i.e., $\Omega = \overline{\gamma}_2 = 30$ dB), a negligible effect is observed in the outage probability (almost the same) since the overall system outage probability is dominated by the weak link, which is the FSO R–D link in this case. The explanation to this behaviour can be given by equation (29) as follows. By using this approximation, the link with the lowest SNR will be dominant and the other term has a minimal effect on the overall system performance.

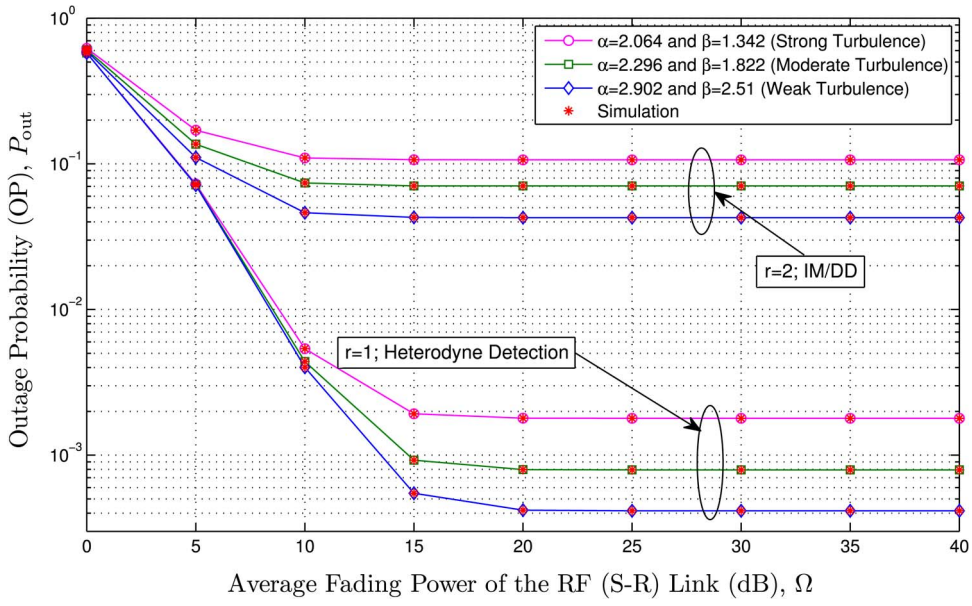

Fig. 11. Average BER of the DBPSK binary modulation scheme showing the performance of the IM/DD technique under strong, moderate, and weak turbulent FSO channels with varying effects of pointing error for the variable gain relay scheme.

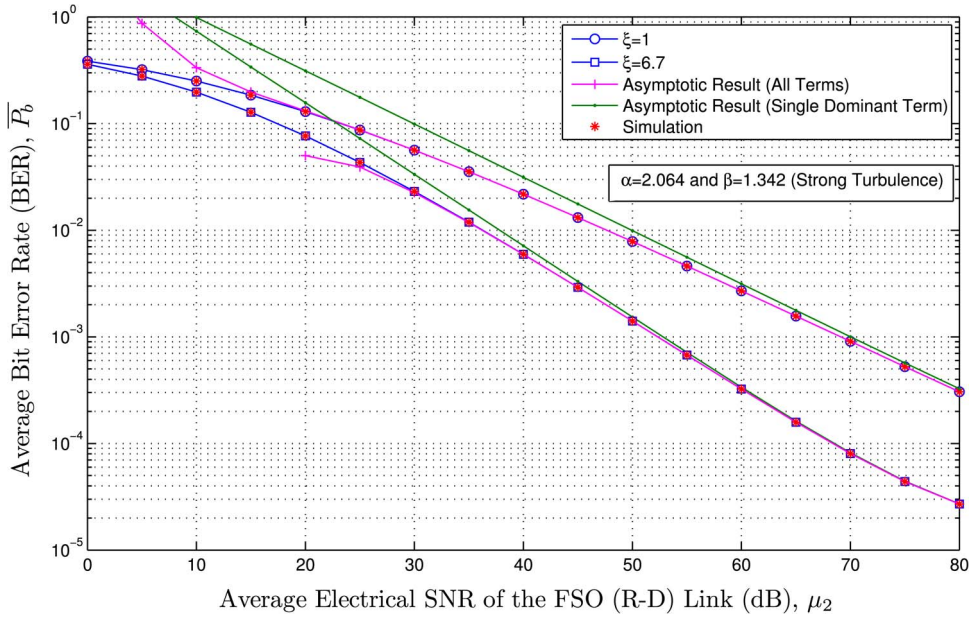

Fig. 12. Average BER of the DBPSK binary modulation scheme showing the performance of the IM/DD technique under strong turbulent FSO channels with varying effects of the pointing error along with the asymptotic results in high SNR regime for $\Omega = 20$ dB for the variable gain relay scheme.

In Fig. 9, the OP for varying effects of the pointing error ($\xi = 1$ and 6.7) under IM/DD technique is presented. We can observe that the performance improves for lower effect of the pointing error (i.e., higher value of ξ, $\xi \to \infty$) and vice versa. Moreover, it can be seen that the OP increases as the atmospheric turbulence conditions get severe. Also, similar results on the average BER can be observed in Figs. 10 and 11 as were seen above in Figs. 8 and 9 for the OP case.

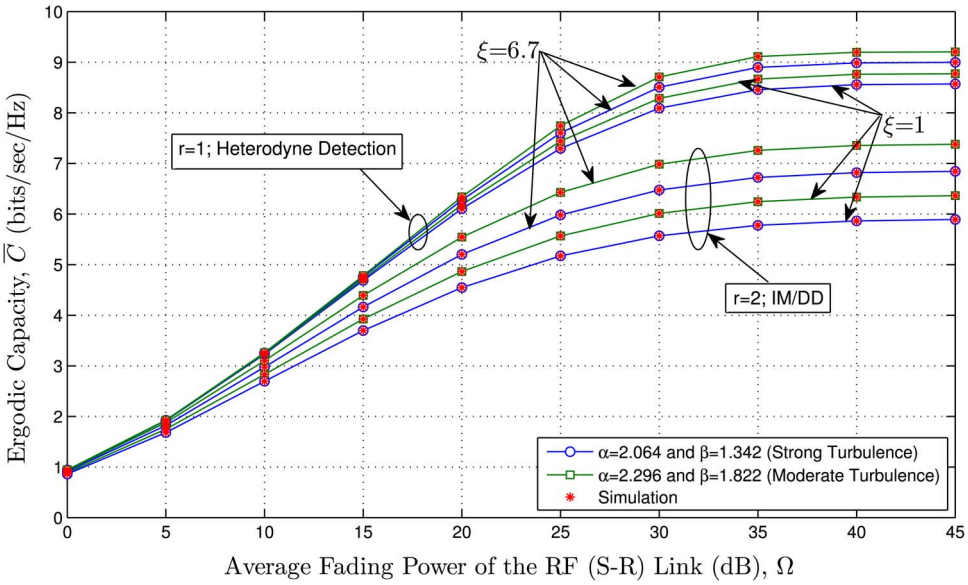

Fig. 13. Ergodic capacity results showing the performance of both heterodyne and IM/DD techniques under strong turbulence conditions for varying pointing errors for the variable gain relay scheme.

Fig. 12 depicts the average BER for DBPSK binary modulation scheme under IM/DD technique for varying effects of the pointing error ($\xi = 1$ and 6.7) along with the asymptotic results at high SNR regime. It can be shown that at high SNR, the asymptotic expression utilizing the Meijer's *G* function expansion and considering all the terms in the summation in (46) converges quite fast to the exact result proving this asymptotic expression to be tight enough. Moreover, if we select the appropriate single dominant term based on the effects of the pointing error and the fading parameters (i.e., α and β), we get also a convergence to the exact result though relatively slower.

In Fig. 13, the ergodic capacity under both heterodyne and IM/DD detection techniques for varying effects of the pointing error ($\xi = 1$ and 6.7) for strong and moderate turbulence conditions is depicted. As expected, it can be seen that heterodyne technique performs better than the IM/DD technique. Also, as the pointing error gets severe and/or the atmospheric turbulence conditions get severe, the ergodic capacity starts dropping.

5. Conclusion

In this paper, we, for the first time, provided unified exact closed-form expressions for the PDF, the CDF, the MGF, and the moments of a dual-hop fixed and variable gain relay systems over the asymmetric links composed of both Nakagami-*m* and unified Gamma–Gamma fading environments. From these formulas, we derived unified expressions for the higher-order AF, the average BER, and the ergodic capacity. In addition, we introduced asymptotic expressions at high SNR regime for the CDF, the MGF, the OP, and the average BER utilizing the Meijer's *G* function asymptotic expansion. We also demonstrated that the system performance degrades as the pointing error effect and/or the atmospheric turbulent conditions become severe.

References

[1] W. Gappmair, "Further results on the capacity of free-space optical channels in turbulent atmosphere," *IET Commun.*, vol. 5, no. 9, pp. 1262–1267, Jun. 2011.
[2] L. C. Andrews, R. L. Phillips, and C. Y. Hopen, *Laser Beam Scintillation With Applications*. Bellingham, WA, USA: SPIE Press, 2001.
[3] W. Popoola and Z. Ghassemlooy, "BPSK subcarrier intensity modulated free-space optical communications in atmospheric turbulence," *IEEE/OSA J. Lightw. Technol.*, vol. 27, no. 8, pp. 967–973, Apr. 2009.

[4] J. Park, E. Lee, and G. Yoon, "Average bit-error rate of the Alamouti scheme in Gamma–Gamma fading channels," *IEEE Photon. Technol. Lett.*, vol. 23, no. 4, pp. 269–271, Feb. 2011.
[5] M. Safari and M. Uysal, "Relay-assisted free-space optical communication," *IEEE Trans. Wireless Commun.*, vol. 7, no. 12, pp. 5441–5449, Dec. 2008.
[6] M. Uysal, J. Li, and M. Yu, "Error rate performance analysis of coded free-space optical links over Gamma–Gamma atmospheric turbulence channels," *IEEE Trans. Wireless Commun.*, vol. 5, no. 6, pp. 1229–1233, Jun. 2006.
[7] S. Arnon, "Optimization of urban optical wireless communication systems," *IEEE Trans. Wireless Commun.*, vol. 2, no. 4, pp. 626–629, Jul. 2003.
[8] S. Arnon, "Effects of atmospheric turbulence and building sway on optical wireless communication systems," *Opt. Lett.*, vol. 28, no. 2, pp. 129–131, Jan. 2003.
[9] H. Sandalidis, T. Tsiftsis, G. Karagiannidis, and M. Uysal, "BER performance of FSO links over strong atmospheric turbulence channels with pointing errors," *IEEE Commun. Lett.*, vol. 12, no. 1, pp. 44–46, Jan. 2008.
[10] T. Tsiftsis, "Performance of heterodyne wireless optical communication systems over Gamma–Gamma atmospheric turbulence channels," *Electron. Lett.*, vol. 44, no. 5, pp. 372–373, Feb. 2008.
[11] C. Liu, Y. Yao, Y. Sun, and X. Zhao, "Average capacity for heterodyne FSO communication systems over Gamma–Gamma turbulence channels with pointing errors," *Electron. Lett.*, vol. 46, no. 12, pp. 851–853, Jun. 2010.
[12] M. Hasna and M.-S. Alouini, "A performance study of dual-hop transmissions with fixed gain relays," *IEEE Trans. Wireless Commun.*, vol. 3, no. 6, pp. 1963–1968, Nov. 2004.
[13] Y. Zhu, Y. Xin, and P.-Y. Kam, "Outage probability of Rician fading relay channels," *IEEE Trans. Veh. Technol.*, vol. 57, no. 4, pp. 2648–2652, Jul. 2008.
[14] S. Datta, S. Chakrabarti, and R. Roy, "Error analysis of noncoherent FSK with variable gain relaying in dual-hop Nakagami-*m* relay fading channel," in *Proc. Int. Conf. SPCOM*, Jul. 2010, pp. 1–5.
[15] G. Karagiannidis, "Performance bounds of multihop wireless communications with blind relays over generalized fading channels," *IEEE Trans. Wireless Commun.*, vol. 5, no. 3, pp. 498–503, Mar. 2006.
[16] E. Lee, J. Park, D. Han, and G. Yoon, "Performance analysis of the asymmetric dual-hop relay transmission with mixed RF/FSO links," *IEEE Photon. Technol. Lett.*, vol. 23, no. 21, pp. 1642–1644, Nov. 2011.
[17] I. S. Ansari, F. Yilmaz, and M.-S. Alouini, "On the performance of hybrid RF and RF/FSO fixed gain dual-hop transmission systems," in *Proc. 2nd SIECPC*, Riyadh, Saudi Arabia, Apr. 2013, pp. 1–6.
[18] I. S. Ansari, F. Yilmaz, and M.-S. Alouini, "On the performance of mixed RF/FSO variable gain dual-hop transmission systems with pointing errors," in *Proc. IEEE 78th VTC*, Las Vegas, NV, USA, Sep. 2013, pp. 1–6.
[19] I. S. Ansari, F. Yilmaz, and M.-S. Alouini, "Impact of pointing errors on the performance of mixed RF/FSO dual-hop transmission systems," *IEEE Wireless Commun. Lett.*, vol. 2, no. 3, pp. 351–354, Jun. 2013.
[20] N. Miridakis, M. Matthaiou, and G. Karagiannidis, "Multiuser relaying over mixed RF/FSO links," *IEEE Trans. Commun.*, vol. 62, no. 5, pp. 1634–1645, Mar. 2014.
[21] M. Simon and M.-S. Alouini, "Digital communication over fading channels," *IEEE Trans. Wireless Commun.*, to be published.
[22] H. Sandalidis, T. Tsiftsis, and G. Karagiannidis, "Optical wireless communications with heterodyne detection over turbulence channels with pointing errors," *IEEE/OSA J. Lightw. Technol.*, vol. 27, no. 20, pp. 4440–4445, Oct. 2009.
[23] H. Nistazakis, T. Tsiftsis, and G. Tombras, "Performance analysis of free-space optical communication systems over atmospheric turbulence channels," *IET Commun.*, vol. 3, no. 8, pp. 1402–1409, Aug. 2009.
[24] M. Feng *et al.*, "Outage performance for parallel relay-assisted free-space optical communications in strong turbulence with pointing errors," in *Proc. Int. Conf. WCSP*, Nov. 2011, pp. 1–5.
[25] H. Li-qiang, W. Qi, and S. Katsunori, "Outage probability of free space optical communication over atmosphere turbulence," in *Proc. WASE ICIE*, Aug. 2010, vol. 4, pp. 127–130.
[26] H. E. Nistazakis, E. Karagianni, A. Tsigopoulos, M. Fafalios, and G. Tombras, "Average capacity of optical wireless communication systems over atmospheric turbulence channels," *IEEE/OSA J. Lightw. Technol.*, vol. 27, no. 8, pp. 974–979, Apr. 2009.
[27] E. Zedini, I. S. Ansari, and M.-S. Alouini, "Unified performance analysis of mixed line of sight RF-FSO fixed gain dual-hop transmission systems," in *Proc. IEEE WCNC*, New Orleans, LA, USA, Mar. 2015, pp. 1–6.
[28] I. S. Gradshteyn and I. M. Ryzhik, *Table of Integrals, Series and Products*. New York, NY, USA: Academic, 2000.
[29] I. S. Ansari, F. Yilmaz, and M.-S. Alouini, "A unified performance of free-space optical links over Gamma–Gamma turbulence channels with pointing errors," *IEEE Trans. Commun.*, Tech. Rep., submitted for publication. [Online]. Available: http://hdl.handle.net/10754/305353
[30] I. Wolfram, *Research, Mathematica Edition: Version 8.0*. Champaign, IL, USA: Wolfram Research, Inc., 2010.
[31] M. D. Springer, *The Algebra of Random Variables (Probability & Mathematical Statistics)*. New York, NY, USA: Wiley, 1979.
[32] A. Prudnikov, Y. Brychkov, and O. Marichev, *Integrals and Series, Volume 3: More Special Functions*. Boca Raton, FL, USA: CRC Press, 1999.
[33] F. Yilmaz and M.-S. Alouini, "Novel asymptotic results on the high-order statistics of the channel capacity over generalized fading channels," in *Proc. IEEE 13th Int. Workshop SPAWC*, 2012, pp. 389–393.
[34] I. S. Ansari *et al.*, "A new formula for the BER of binary modulations with dual-branch selection over generalized-K composite fading channels," *IEEE Trans. Commun.*, vol. 59, no. 10, pp. 2654–2658, Oct. 2011.
[35] N. Sagias, D. Zogas, and G. Karagiannidis, "Selection diversity receivers over nonidentical Weibull fading channels," *IEEE Trans. Veh. Technol.*, vol. 54, no. 6, pp. 2146–2151, Nov. 2005.
[36] A. Lapidoth, S. Moser, and M. Wigger, "On the capacity of free-space optical intensity channels," *IEEE Trans. Inf. Theory*, vol. 55, no. 10, pp. 4449–4461, Oct. 2009.
[37] S. Arnon *et al.*, *Advanced Optical Wireless Communication Systems*. Cambridge, U.K.: Cambridge Univ. Press, 2012. [Online]. Available: http://dx.doi.org/10.1017/CBO9780511979187
[38] A. Annamalai, R. Palat, and J. Matyjas, "Estimating ergodic capacity of cooperative analog relaying under different adaptive source transmission techniques," in *Proc. IEEE Sarnoff Symp.*, Apr. 2010, pp. 1–5.

[39] A. Mathai and R. Saxena, *The H-function With Applications in Statistics and Other Disciplines*. New York, NY, USA: Wiley, 1978.
[40] S. Ikki and S. Aissa, "Performance evaluation and optimization of dual-hop communication over Nakagami-*m* fading channels in the presence of co-channel interferences," *IEEE Commun. Lett.*, vol. 16, no. 8, pp. 1149–1152, Aug. 2012.
[41] S. Ikki and S. Aissa, "A study of optimization problem for amplify-and-forward relaying over Weibull fading channels with multiple antennas," *IEEE Commun. Lett.*, vol. 15, no. 11, pp. 1148–1151, Nov. 2011.
[42] S. Gupta, "Integrals Involving Products of *G*-functions," in *Proc. Nat. Acad. Sci. India*, 1969, pp. 539–542.
[43] X. Tang, Z. Ghassemlooy, S. Rajbhandari, W. Popoola, and C. Lee, "Coherent polarization shift keying modulated free space optical links over a Gamma–Gamma turbulence channel," *Amer. J. Eng. Appl. Sci.*, vol. 4, no. 9, pp. 520–530, 2011.